Fluorescence, Phosphorescence, and Optically Detected Magnetic Resonance Studies of the Nucleic Acid Association of the Nucleocapsid Protein of the Murine Leukemia Virus[†,‡]

Jie Q. Wu,[§] August H. Maki,*[,§] Andrzej Ozarowski,[§] María Angeles Urbaneja,[||] Louis E. Henderson,[||] and José R. Casas-Finet[||]

Department of Chemistry, University of California, Davis, California 95616, and AIDS Vaccine Program, SAIC Frederick National Cancer Institute-Frederick Cancer Research and Development Center, Frederick, Maryland 21702-1201

Received December 2, 1996; Revised Manuscript Received February 21, 1997[⊗]

ABSTRACT: Fluorescence, phosphorescence, and optical detection of triplet state magnetic resonance (ODMR) are employed to investigate the interaction of p10, the nucleocapsid protein of the Moloney murine leukemia virus, with nucleic acids. p10 is a 55-amino acid protein containing a single zinc finger motif, $C^{26}C^{29}H^{34}C^{39}$, that includes Y at position 28 and W at position 35. In addition, the interactions of a zinc finger peptide, p10-ZF, comprising residues 24−41 of p10, and a doubly mutated 24−41 peptide, p10-ZF′ in which the positions of Y and W are interchanged, also are reported. The measurements focus on the direct involvement of the sole W residue in the nucleic acid interaction. Fluorescence quenching and salt-back titrations indicate complex formation of p10 with several octanucleotides—$(dT)_8$, $(dI)_8$, $(dU)_7dT$, and $(5\text{-BrdU})_7dT$—and with the polynucleotides poly(dT) and poly(dI). Poly(dI) binds with the highest affinity. Apparent binding constants and salt-back midpoints are reported. Neither p10-ZF nor p10-ZF′ exhibits significant fluorescence quenching by these DNA substrates. Binding of p10-ZF to fluorescent poly(ethenoadenylic acid) was detected with greatly reduced affinity relative to p10, but binding of p10-ZF′ was undetectable. These results are in general agreement with phosphorescence and ODMR measurements monitoring W. Addition of poly(I) to p10 leads to a phosphorescence red shift, reduction in the zero-field splitting (ZFS) parameters *D* and *E*, and a significantly reduced phosphorescence lifetime, each consistent with aromatic stacking interactions between W and the nucleobases. These effects are smaller with p10-ZF and undetectable with p10-ZF′. Poly(U) produces no significant changes in the triplet state parameters of W; no stacking interactions are observed even for p10. $(5\text{-BrdU})_7dT$ yields large phosphorescence red shifts in p10 and p10-ZF, and reductions of *D*, but no significant heavy atom effects. These effects probably are due to enhanced local polarizability caused by Br, but any stacking interactions in these complexes would exclude van der Waals contacts between W and the Br atoms.

Retroviral nucleocapsid (NC)[1] proteins are synthesized as a domain in the Gag polyprotein precursor and are released by the action of the viral protease during the maturation process. In general, mature NC proteins are small (50−70 residues), highly basic (p*I* of greater than 9) proteins that bind to single-stranded nucleic acids (Long et al., 1980). NC proteins of all known retroviruses (except members of the Spumavirus class) have one or two copies of a highly conserved amino acid sequence consisting of 10 variable residues (X) and 4 invariant residues, $Cys\text{-}(X)_2\text{-}Cys\text{-}(X)_4\text{-}His\text{-}(X)_4\text{-}Cys$. The invariant residues function to coordinate zinc through histidine imidazole and cysteine thiolates, forming CCHC-type zinc fingers (Berg, 1986; Bess et al., 1992). The nucleocapsid protein isolated from HIV-1 particles binds Zn(II) and forms retroviral-type zinc fingers (Summers et al., 1992). The CCHC zinc fingers provide the Gag precursors and the mature NC proteins with a highly organized structure that facilitates nucleic acid binding.

Much of our current understanding of the biological functions of retroviral NC proteins has come from the analysis of viruses constructed with point mutations in the CCHC zinc finger regions of the protein. Model viruses for these studies include the Moloney murine leukemia virus (MoMuLV) which has one CCHC zinc finger per NC protein (Henderson et al., 1981, 1984) and HIV-1 which has two CCHC zinc fingers per NC protein (Henderson et al., 1992). Point mutations replacing the Cys thiolate sulfur with oxygen or hydrogen (i.e., C to S or A mutations) prevent zinc binding and destabilize the zinc finger peptide conformation in the Gag precursor and in the NC protein (Gorelick et al., 1988,

[†] This research was partially supported by NIH Grant ES-02662 (A.H.M.). M.A.U. is a recipient of a fellowship from the Subdirección General de Promoción de la Investigación, Ministerio de Educación y Ciencia (Spain).

[‡] The content of this publication does not necessarily reflect the views or policies of the Department of Health and Human Services, nor does mention of trade names, commercial products, or organizations imply any endorsement by the U.S. Government.

* Author to whom correspondence should be addressed.

[§] University of California.

[||] SAIC Frederick National Cancer Institute-Frederick Cancer Research and Development Center.

[⊗] Abstract published in *Advance ACS Abstracts,* May 1, 1997.

[1] Abbreviations: EDTA, ethylenediaminetetraacetate; EG, ethylene glycol; HIV-1, human immunodeficiency virus type 1; k_i, decay rate constant of the T_i ($i = x, y,$ or z) sublevel of the triplet state; MoMuLV, Moloney murine leukemia virus; NC, nucleocapsid; ODMR, optically detected magnetic resonance; p7, nucleocapsid protein of HIV-1; p10, MoMuLV nucleocapsid protein; p10-ZF, 18-residue MoMuLV p10 zinc finger peptide (residues 24−41); p10-ZF′, p10-ZF Y28W/W35Y (an 18-residue MoMuLV p10 zinc finger peptide spanning residues 24−41 and carrying transposed Tyr and Trp aromatic side chains); poly(ϵA), poly(1-N^6-ethenoadenylic acid); SLR, spin−lattice relaxation; ZFS, zero-field splittings.

S0006-2960(96)02951-0 CCC: $14.00

1991; Mçric et al., 1989). In general, these mutants are defective in RNA packaging (i.e., less than 10% of wild-type levels of viral RNA) and are at least 6 orders of magnitude less infectious than the wild-type virus. These C to S or A mutants constitute dramatic proof of the RNA recognition and packaging role of the NC domain in the Gag precursor. However, the fact that these mutants are even more defective in infectivity than they are in RNA packaging suggests additional biological roles for NC zinc fingers (Gorelick et al., 1988; Darlix et al., 1995). After maturation (proteolytic cleavage), the mature NC protein remains bound to the RNA and forms the RNA−protein complex in the core of the infectious virus. During the infectious process, the NC protein remains bound to the RNA in the preintegration complex (Gallay et al., 1995). Recently, the importance of the NC protein in the infectious process was underscored by the phenotype of viruses with point mutations that replace Cys with His (i.e., CCHC to CCHH) (Gorelick et al., 1996) or exchange the positions of the zinc fingers in p7, the HIV-1 NC protein (Gorelick et al., 1993). These mutants retain the ability to bind zinc, undergo normal assembly and budding, package wild-type levels of genomic RNA, and form mature particles but are nevertheless 4−6 orders of magnitude less infectious than the wild-type virus. The CCHH and CCCC mutants clearly demonstrate that wild-type zinc fingers in the mature NC protein are required for the infectious process. These *in vivo* results are supported by *in vitro* studies showing that purified NC protein can facilitate reactions catalyzed by the viral reverse transcriptase (Ji et al., 1996; Pellska et al., 1994; Tsuchihashi & Brown, 1994), including primer binding, strong stop synthesis, strand transfer (DeStefano, 1995; Rodriguez-Rodriguez et al., 1995; You & McHenry, 1994), and processivity (DeStefano et al., 1992). In addition, many studies indicate that retroviral NC proteins can function as nucleic acid chaperones by facilitating annealing (Khan & Giedroc, 1992; Lapadat-Tobolsky et al., 1995) and conformational rearrangements (Herschlag et al., 1994; Dib-Haij et al., 1993) in a non-sequence-dependent fashion. This sequence-independent activity does not show an absolute requirement for zinc fingers and seems mediated primarily through ionic interactions involving basic amino acids (Prats et al., 1991; Schmalzbauer et al., 1996). Thus, a growing body of evidence is showing that the NC protein (or domain in the Gag precursor) functions in the management of nucleic acids during almost every stage of the viral replication cycle.

Single-stranded nucleic acid interactive proteins often involve aromatic side chains in hydrophobic (stacking) interactions with exposed nucleic acid bases. Among the aromatic amino acids, tryptophan has been shown to result in the largest stabilization energy as a result of intercalation (Kumar & Govil, 1984). The luminescence properties of the indole ring have been used in the characterization of a large number of single-stranded nucleic acid binding proteins. In particular, optically detected magnetic resonance (ODMR) is a technique [for reviews, see Maki (1984) and Hoff (1989)] especially well-suited to assessing the occurrence of aromatic intercalation of Trp side chains with nucleobases. Aromatic stacking interactions have been demonstrated by the application of ODMR techniques in a number of nucleic acid interactive systems that exhibit preferential binding to single-stranded lattices. Among these are the NC protein p7 from HIV-1 (Lam et al., 1994), gene 32 protein from bacteriophage T4 (Khamis & Maki, 1986; Casas-Finet et al., 1988a), *Escherichia coli* single-stranded DNA binding protein (SSB) (Casas-Finet et al., 1987), various SSB point mutations replacing its Trp residues (Khamis et al., 1987; Zang et al., 1987; Tsao et al., 1989), and an IncY plasmid-encoded SSB from *E. coli* (Casas-Finet et al., 1988b). Stacking interactions also are indicated by thermodynamic studies of nucleic acid binding by oligolysines that incorporate Trp residues (Mascotti & Lohman, 1993) and by ODMR studies of Lys-Trp-Lys interactions with RNA (Co & Maki, 1978).

Previous ODMR measurements have shown (Tsao et al., 1989; Maki, 1995, and references cited therein) that the zero-field splitting (ZFS) parameters of Trp are sensitive to changes in the local environment. In addition, aromatic stacking interactions exhibited by the quinoxaline chromophores of the bis-intercalating antibiotic echinomycin and the quinoline chromophores of its analog 2QN when bound to DNA are characterized (Alfredson et al., 1991; Maki et al., 1992) by a reduction in the ZFS parameter, *D*, that correlates linearly with the free energy of binding to differing DNA base sequences. This correlation suggests that the London dispersion interactions that accompany the stacking of aromatic residues in these complexes contribute significantly to the binding energy, influence the selectivity of binding, and contribute to a reduction in the ZFS parameter, *D*. Furthermore, the triplet state decay constant increases with intercalation, and the phosphorescence spectrum undergoes a red shift.

In previous phosphorescence and ODMR measurements on p7, the NC protein from HIV-1 which contains two zinc finger regions, one of which carries the sole Trp residue, we have found (Lam et al., 1993, 1994) similar effects upon RNA binding. The phosphorescence 0,0-band of Trp is shifted to the red by 5.9 nm when poly(I) is bound, by 4.4 nm when poly(G) or $(dG)_8$ is bound, by 1.8 nm when poly(U) is bound, and by 1.4 nm when poly(C) is bound. These red shifts correlate with the binding affinities to the homooligomers, $(dI)_8 > (dG)_8 > (dU)_8 > (dC)_8$. In addition, slow-passage ODMR measurements on p7 revealed energy reductions in the *D* parameter of ca. 100 MHz upon binding to poly(I), ca. 40 MHz with $(dG)_8$, and ca. 30 MHz with poly(U). These shifts could not be measured accurately because of a severe degradation of ODMR signal intensity that accompanies nucleic acid binding to p7. Work (J. Q. Wu, unpublished results) using newly developed experimental and analysis methods (described below) to measure these shifts in p7 with greater accuracy is in progress. The apparent triplet state sublevel decay constants of Trp also increase when these nucleic acids bind to p7. These effects provide evidence for the presence of Trp stacking with bases when p7 is bound to these nucleic acid substrates and suggest that aromatic stacking of Trp takes place in the binding of the zinc finger to RNA.

In this paper, we report on phosphorescence and ODMR measurements of p10, p10-ZF, and p10-ZF′ and the effects of binding these peptides to various nucleic acids on the triplet state properties of the Trp residue. We have employed a newly developed (Wu et al., 1996b) delayed slow-passage ODMR experiment and the associated analysis of the signal that compensates for fast passage effects on the band shape. Thus, the analysis yields the correct ODMR band center frequency and band width. The delayed slow-passage experiment generally results in enhanced signal intensity

relative to the conventional slow-passage ODMR measurements carried out in the photostationary state. This turns out to apply in particular to p10, in which perturbations of the triplet state kinetic parameters upon nucleic acid binding reduce the spin alignment (sublevel population differences) in the photostationary state that is an absolute requirement for the observation of ODMR signals. The ODMR measurements of triplet state properties are compared with binding affinity measurements using fluorescence quenching and salt-back titrations.

The work reported here leads to the major conclusion that aromatic stacking interactions of Trp accompany poly(I) binding to p10 and that the stacking interactions are weaker when p10-ZF binds to this polynucleotide. On the other hand, evidence of aromatic stacking of Trp is not found in complexes of p10-ZF′ with any nucleic acids investigated, in agreement with its very poor nucleic acid binding affinity as measured from fluorimetric equilibrium binding isotherms. Effects observed in the binding of poly(U) are less pronounced and are attributed to either marginal stacking or nonspecific environmental perturbations. Interaction of each peptide with $(5\text{-BrdU})_7$dT leads to a red shift in the phosphorescence, but only minor external heavy atom effects or other perturbations of the triplet state occur, suggesting that aromatic stacking, if present, does not involve van der Waals contact between the Br atom of 5-BrU and Trp. It suggests that a nonspecific increase of local polarizability due to the Br atom is responsible in each case for the red shift of the Trp phosphorescence and minor reduction of the ZFS.

MATERIALS AND METHODS

p10 was isolated from purified MoMuLV viral suspensions by reversed phase HPLC as previously described (Henderson et al., 1984). HPLC fractions containing peptide (identified by PAGE mobility, Western blotting, and N-terminal sequencing) were collected, pooled, and lyophilized. The peptide was resuspended in the presence of excess Zn(II), and its concentration was calculated on the basis of optical absorbance and amino acid analysis measurements. Metal uptake was verified by EDTA competition monitoring the evolution of Trp fluorescence. This solution was aliquoted into sterile polypropylene vials and relyophilized. The p10 sequence has been determined (Shinnick et al., 1981) to be ATVVSGQKQD^{10}RQGGERRRSQ^{20}LDRDQCAYCK^{30}-EKGHWAKDCP^{40}KKPRGPRGPR^{50}PQTSLL. The sequences of the zinc finger peptides studied in the present work are D^{24}QCAYCKEKGHWAKDCPK^{41} (p10-ZF) and D^{24}QC-AWCKEKGHYAKDCPK^{41} (p10-ZF′). These peptides were obtained from Macromolecular Resources, Inc. (Fort Collins, CO). Poly(U) and poly(I) were purchased from Pharmacia, Inc., while poly(ϵA) was obtained from P. L. Biochemicals. The oligodeoxynucleotides were synthesized by the Recombinant DNA Laboratory, SAIC Frederick (Frederick, MD) using Glen Research phosphoramidite precursors, size-purified by gel electrophoresis, and electroeluted. Concentrations of nucleic acids were obtained spectrophotometrically, using $\epsilon_{249} = 12\,700$ M^{-1} cm^{-1}, $\epsilon_{260} = 7400$ M^{-1} cm^{-1}, $\epsilon_{264} = 8520$ M^{-1} cm^{-1}, and $\epsilon_{278} = 6900$ M^{-1} cm^{-1} for poly(I), poly(U), poly(dT) (Sigma Molecular Biology 1996/1997 Catalog), and $(5\text{-BrdU})_7$dT (Michelson et al., 1962), respectively.

Binding affinities of p10 protein and peptides for the various DNA oligo- and polynucleotides used in this study were obtained by following the Trp fluorescence emission intensity in the presence of various concentrations of the macromolecule. Fluorescence measurements were carried out on either a Shimadzu RF 5000U or a SPEX Fluoromax spectrofluorimeter, with excitation at 288 nm (1 nm band width) and emission at 353 nm (5 nm band width). Equilibrium binding isotherms were acquired at 25 °C, following stepwise additions of a concentrated nucleic acid solution to a 0.4 mL p10 sample (0.78 μM) in 10 mM sodium phosphate buffer (pH 7.0) placed in a Teflon-capped, dual (0.2 × 1.0 cm) path length Suprasil quartz cell (Uvonic). Readings were taken every 5 s for 2 min, averaged, and corrected for dilution and inner filter effects. Salt-back titrations were carried out upon addition of a concentrated NaCl solution to a preformed p10−nucleic acid complex. Double-logarithmic plots of log K_{app} *vs* log[Na$^+$] were used to derive binding constants at various ionic strength conditions. Binding to RNA was monitored by the increase of the fluorescence of the homopolymeric poly(ϵA) lattice upon additions of concentrated p10 protein or zinc finger peptide solutions. Excitation was at 315 nm (1 nm band width) to avoid interference from tryptophan absorption, and emission was detected at 400 nm (5 nm band width). Salt-back titrations were also carried out with these samples.

For phosphorescence and ODMR measurements, peptide samples were dissolved in ethylene glycol (EG)−10 mM sodium phosphate buffer at pH 7.0 (30% v/v). Final peptide concentrations ranged between 0.1 and 0.5 mM. Complexes with nucleic acids were formed at ambient temperature by progressive addition of aliquots of concentrated peptide solution while mixing. The nucleic acid phosphate concentration of poly(U) and poly(I) was approximately 20 times that of the peptide. In the case of $(5\text{-BrdU})_7$dT, the ratio was about 11 to minimize the 5-BrU phosphorescence background. Solutions were allowed to stand at ambient temperature for at least 10 min prior to cooling and acquiring phosphorescence and ODMR spectra. Phosphorescence measurements were made at 77 K. The sample temperature was reduced to 1.2 K by immersion in pumped liquid He for ODMR measurements. Samples were ca. 10 μL contained in a 1 mm inside diameter Suprasil quartz tube inserted into a Cu slow-wave helix that terminated a 50 Ω microwave transmission line. Details of the ODMR spectrometer have been described recently (Wu et al., 1996a), but it has been modified somewhat. Photon counting is employed for both phosphorescence and ODMR measurements. The cooled photomultiplier (EMI, Inc., model 6256) output pulses are amplified by a fast preamplifier, followed by an amplifier-discriminator (Ortec, Inc., models 9301 and 9302, respectively). The NIM standard negative current pulses from the discriminator are fed to a multichannel scaler board (EG&G Ortec, Inc., MCS-plus) located in a 486 personal computer, where signal averaging is carried out.

In this paper, we present the results of two types of slow-passage ODMR measurements in which the phosphorescence intensity is monitored while slowly sweeping the microwave frequency through a zero-field magnetic resonance transition.

The first of these is the traditional experiment carried out during continuous optical pumping. We have shown recently (Wu et al., 1996a) how to analyze the responses using a theory that compensates for unavoidable rapid-passage

Table 1: Binding Parameters of MoMuLV NC Protein (p10) to DNA Octanucleotides and Polynucleotides

ligand	salt-back midpoint (mM Na^+)	K_{app}[a]
$(dT)_8$	17	8.7×10^4
poly(dT)	52	4.3×10^6
$(dI)_8$	51	1.9×10^6
poly(dI)	91	6.7×10^7
$(dU)_7dT$	9.8	1.9×10^4
$(5Br\text{-}dU)_7dT$	11.3	3.0×10^5

[a] Measurements carried out in a 13 mM NaCl solution.

distortions of the band shape. The observed responses are fitted to the theoretical model using a Marquardt−Levenberg procedure that minimizes the χ^2 of the data set. The parameters fitted by this procedure are the true band center frequency, ν_0, the half-width of the band (assumed Gaussian) at half-maximum intensity, $\nu_{1/2}$, the apparent sublevel decay constants for the $T_i \leftrightarrow T_j$ transition, k_i and k_j (i and $j = x$, y, or z), and the relative radiative rate constant, $R_{ji} = k_j^{(r)}/k_i^{(r)}$.

The second type of slow-passage experiment (delayed slow passage) is carried out during decay of the phosphorescence. The response that is analyzed (Wu et al., 1996b) by an analogous Marquardt−Levenberg procedure is the decay curve containing the slow-passage response from which has been subtracted the decay curve in the absence of the microwave-induced response. The parameters that are fitted are the same as those listed above for the slow-passage response during optical pumping. Both types of responses are analyzed assuming that spin−lattice relaxation (SLR) (as well as the kinetic effects of optical pumping in the former experiment) can be neglected. Consequently, the kinetic rate constants, k_i, k_j, and R_{ji}, are referred to as "apparent" rate constants that may be influenced to some extent by residual SLR.

The delayed slow-passage method has some major advantages relative to measurements made during optical pumping. (a) Fluorescence is absent, so a rotating sector with its induced fluctuations can be eliminated. (b) The phosphorescence background is reduced relative to the photostationary state experiment. (c) Population differences between triplet sublevels during decay often are greater than in the photostationary state, leading to improved signal/noise. (d) The kinetic parameters are not affected by the optical pumping rate. In each experiment, measurements are made at several sweep rates (and delay times for the delayed slow-passage experiment), and the data sets are analyzed independently. The standard deviation of a measurement is estimated readily from the variation of the individual best-fit parameters between the independent data sets.

RESULTS

Fluorescence Titrations. The binding affinity of MoMuLV NC protein p10 was determined for various DNA lattices of different lengths and compositions. Binding stoichiometries (oligo/NC) for short oligonucleotides used in this study were 1/1 for each octanucleotide and 2/1 for each tetranucleotide. These values are in agreement with the occluded site size (6 ± 1 bases per NC protein) determined for long polynucleotides from reverse titrations under near-stoichiometric conditions (data not shown). p10 affinity for homodeoxyoctanucleotides ranged from ca. 2×10^4 M^{-1} for U (Table 1) to 5×10^6 M^{-1} for G (not shown), with a base preference ranking of U < T < I < G. Substitution of 5-BrdU for dU resulted in a moderate (15-fold) increase of the binding affinity toward p10 (Table 1). The polynucleotides used in this study, poly(dT) and poly(dI), bound p10 with a K_{app} of ca. 4×10^6 and 7×10^7 M^{-1}, respectively (Table 1). A similar ionic dependence of the binding affinity on monovalent ion concentration was derived from analysis of salt-back titrations (not shown) for all oligonucleotides except $(5\text{-BrdU})_7dT$ (see Discussion). Thus, midpoints of complex disruption with added NaCl reflected closely the ranking of affinities obtained from fluorimetric titrations in which nucleic acid lattice was added to the protein (or peptide). Binding to long polynucleotide chains occurred with a binding affinity about 40 times higher than that for binding to the respective octanucleotides (Table 1). Under the conditions of the ODMR experiments, p10 protein would be expected to be quantitatively bound to the ligand used.

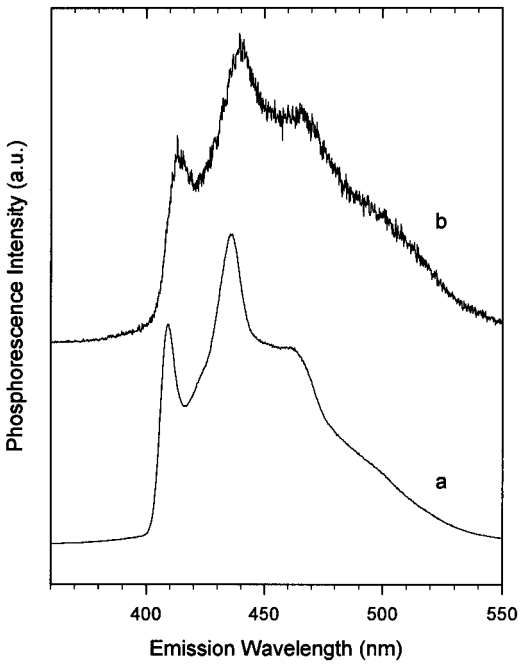

FIGURE 1: Phosphorescence spectra of (a) p10 (0.18 mM) and (b) p10 (0.11 mM) complexed with poly(I) (2.2 mM PO_4) in 30% v/v EG buffer at 77 K. Samples are excited at 295 nm with a 16 nm band-pass.

Neither p10-ZF nor p10-ZF′ exhibited significant quenching of Trp emission in the presence of the DNA lattices mentioned above. The fluorescent polynucleotide, poly(ϵA), was therefore used to assess the binding affinity for these peptides relative to full length p10. Poly(ϵA) usually exhibits enhanced affinity toward single-stranded nucleic acid binding proteins due to its extended nucleic acid moiety comprising a fused three-ring system. p10-ZF experienced a significant decrease in affinity (2.8×10^4 M^{-1}) relative to p10 (2.3×10^7 M^{-1}), whereas binding of the Tyr/Trp-transposed p10-ZF′ peptide was undetectable. These results are in agreement with the magnitude of spectroscopic effects observed in the ODMR experiments (see below).

Phosphorescence Spectra. The phosphorescence spectrum of p10 is compared with that of its poly(I) complex in Figure 1. The phosphorescence red shift and loss of resolution upon complex formation are readily apparent. The poorer signal quality of the complex suggests a reduction in quantum yield, but quantitative measurements were not attempted. In

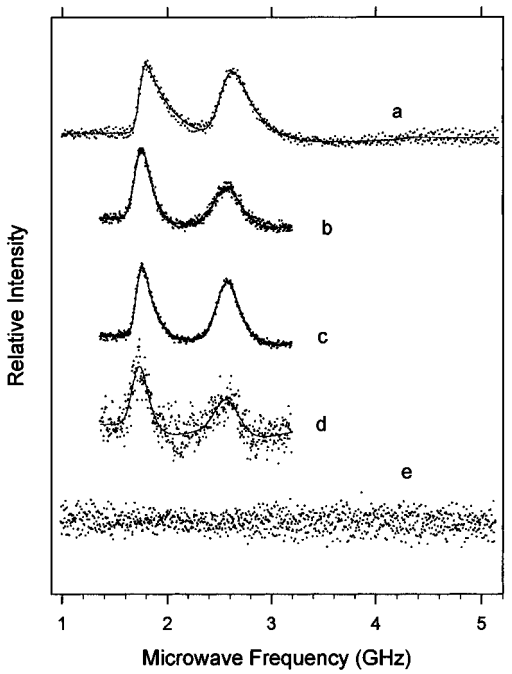

FIGURE 2: Conventional phosphorescence-detected slow-passage ODMR spectra of Trp in (a) p10-ZF (0.44 mM), (b) p10-ZF (0.27 mM) complexed with poly(U) (3.6 mM PO_4), (c) p10 (0.18 mM), (d) p10 (0.14 mM) complexed with poly(U) (3.6 mM PO_4), and (e) p10 (0.11 mM) complexed with poly(I) (2.2 mM PO_4). The solvent is 10 mM aqueous sodium phosphate (pH 7) containing 30% v/v EG, and $T = 1.2$ K. The phosphorescence is monitored at the 0,0-band peak wavelength given in Table 3 using a 3 nm band width, and excitation is at 295 nm using a 16 nm band-pass. The microwave sweep rate is 100 MHz/s for parts a and e and 45 MHz/s for parts b−d. Signal averaging (50−90 accumulations) was carried out to improve signal/noise. Solid curves in parts a−d are best fits calculated using the theory given in Wu et al. (1996a).

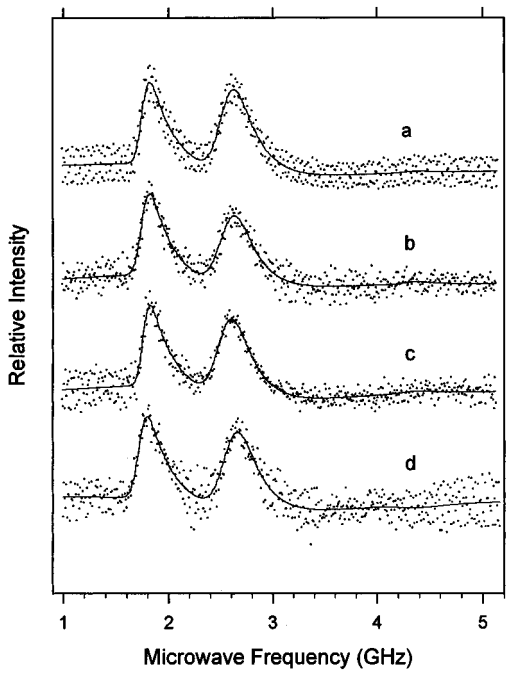

FIGURE 3: Conventional slow-passage ODMR spectra of Trp in p10-ZF′. Experimental conditions are the same as those presented in the Figure 2 caption, except as noted below: (a) p10-ZF′ (0.44 mM), (b) p10-ZF′ (0.26 mM) complexed with poly(U) (5.8 mM PO_4), (c) p10-ZF′ (0.18 mM) complexed with poly(I) (3.6 mM PO_4), and (d) p10-ZF′ (0.09 mM) complexed with $(5\text{-BrdU})_7$dT (1 mM PO_4). The microwave frequency was swept at 100 MHz/s in each case, and signal averaging (40−70 accumulations) was carried out. Solid curves are best fits calculated using the theory of Wu et al. (1996a). Most of the noise in the spectra is coherent, from unaveraged rotating sector modulation.

previous phosphorescence and ODMR measurements on p10 from MuLV (Casas-Finet et al., 1988c), the spectral resolution was much poorer than that which we observe with the present sample. Although the MuLV previously studied was the Rauscher strain, whose sequence differs somewhat from the Moloney strain studied here (Henderson et al., 1981), we believe that the poorer quality of the earlier spectra may have been due in part to sample oxidation and/or denaturation.

Conventional Slow-Passage ODMR Spectra. Some representative examples of conventional slow-passage ODMR spectra are given in Figure 2. Superimposed on the spectra are calculated responses (Wu et al., 1996a) that compensate for fast-passage effects, as discussed in the previous section. Since the spectra are obtained during continuous optical pumping, a rotating sector was employed to eliminate fluorescence; much of the "noise" present in the data points is due to the incompletely signal-averaged intensity fluctuations produced by the sector. The effect of complexing of p10-ZF with poly(U) on the ODMR spectrum is readily apparent from visual comparison of spectrum b with a. Both the $D - E$ (low-frequency) and $2E$ (high-frequency) transitions are shifted to lower frequencies. Complexing of p10 with poly(U) (spectrum d *vs* c) leads to a significant loss of signal/noise. Complexing with poly(I) leads to photostationary state ODMR signal levels that are undetectable (spectrum e). This loss of signal intensity on polynucleotide binding is partially recovered in the delayed slow-passage spectra, to be discussed below, and it is these spectra that have been analyzed (Wu et al., 1996b) in this paper. Complexing of p10-ZF with poly(I) also leads to a significant loss in conventional slow-passage ODMR signal intensity (spectrum not shown).

The effect of adding polynucleotides to p10-ZF′ (in which the positions of Y and W are interchanged) is shown in the conventional slow-passage spectra presented in Figure 3. Incomplete averaging of rotating sector fluctuations is particularly evident in these spectra. In contrast with p10, and p10-ZF, little if any effect of polynucleotide on either the signal level or the resonance frequencies is evident. Any effects of polynucleotides on the triplet state parameters were obtained from analysis of the delayed slow passage spectra, to be discussed below.

Delayed Slow-Passage ODMR Results. Even though the slow-passage ODMR signals of p10 complexed with poly(I) were too weak to be observed in the photostationary state (Figure 2e), they could be observed and analyzed in a delayed slow-passage experiment. The $D - E$ and $2E$ signals of p10 complexed with poly(I) are shown in Figure 4. The $D - E$ signal was measured using three different microwave sweep rates, while two different sweep rates were used for the measurement of the $2E$ transition. These slow-passage signals and those of the other samples investigated in this work were analyzed (Wu et al., 1996b); the best-fit parameters were averaged for each transition, and these averaged parameters are reported in Tables 2 and 3, along with their standard deviations (σ). In Table 3, we also report the phosphorescence 0,0-band peak wavelengths and deconvolution of the decay at 77 K. The vertical dashed lines in

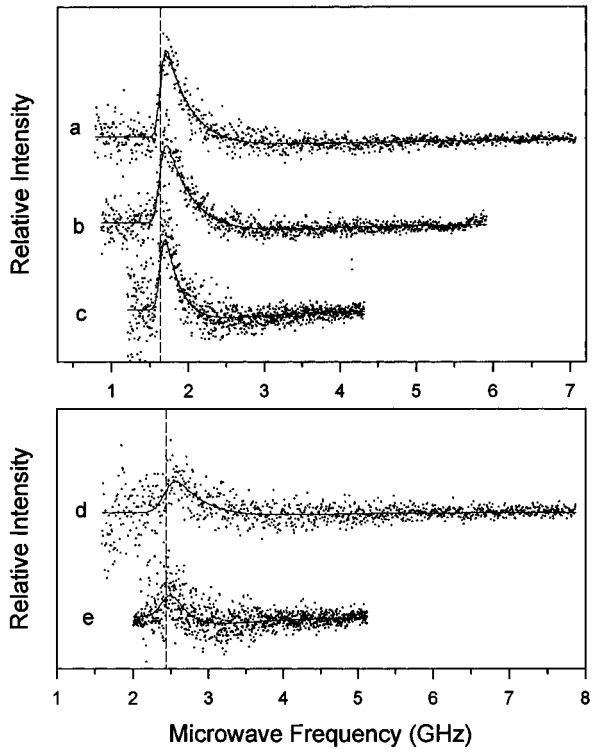

FIGURE 4: Delayed slow-passage ODMR spectra of Trp in p10 complexed with poly(I). Sample and excitation/emission conditions are given in the Figure 2 caption and Table 3. The $D - E$ transition is shown above with microwave sweep rates of (a) 200, (b) 160, and (c) 100 MHz/s; the $2E$ transition is shown below with microwave sweep rates of (d) 200 and (e) 100 MHz/s. The microwave frequency output is limited by a 2 GHz low-pass filter for parts a−c and by a 3 GHz low-pass filter for parts d and e. Signal averaging (42−86 accumulations) was carried out. The solid curves are the calculated nonlinear least-squares best fits to the responses from the theory given in Wu et al. (1996b), using the parameters listed in Tables 2 and 3. The vertical dashed lines are the average values of ν_0 for the $D - E$ transition (above) and for the $2E$ transition (below) given in Table 2.

Figure 4 are the average best-fit values of ν_0 for these transitions taken from Table 2.

DISCUSSION

The measurements reported in this paper have been carried out with the aim of utilizing fluorescence measurements and detailed triplet state properties of the single Trp residue of p10, p10-ZF, and p10-ZF′ to obtain information about the involvement of the zinc finger in nucleic acid binding.

Fluorescence Titrations. Among short DNA homopolymeric octanucleotides, uracil and thymine lattices bound with similar affinities. 5-BrdU showed a measurable increase in its binding constant relative to the previous sequences. Its salt dependence, however, also became steeper as reflected by a salt-back midpoint intermediate between that of U and T. We suggest that these effects may stem from an increase in average 5-BrdU/5-BrdU base distance as a result of steric hindrance of the bulky halogen substituent. The ensuing destacking of nucleic acid bases would reduce the energetic penalty term involved in the intercalation of an aromatic amino acid side chain. The higher apparent affinity of long polynucleotide lattices relative to single-site ligands could result either from a cooperative effect in the binding process or from a dissimilar salt dependence of their interaction with p10 resulting from the different counterion density around the polyphosphate chain that is expected for oligos (due to end effects) relative to polynucleotides. A detailed account of the thermodynamic properties of wild-type and point-mutated p10 protein will be published elsewhere.

Involvement of charged residues located outside the zinc finger domain is inferred from the drop in affinity toward poly(ϵA) of 3 orders of magnitude resulting from truncation of the p10 sequence. Swapping of the aromatic residues within the zinc finger results in a drastic loss of binding affinity for nucleic acids. This double-point mutation does not induce ejection of the chelated metal ion (P. Nower and J. R. Casas-Finet, unpublished results). It is conceivable, however, that exchange of the phenol and indole groups could affect nucleic acid binding through a local distortion of the peptide backbone structure. An alignment of primary sequence data from structural data bases shows that in all instances NC proteins that carry a single zinc finger have a Phe or Tyr residue in the shorter first loop of the finger while Trp is absolutely conserved in the third loop. These retrovirus families cover a relatively broad genus range among vertebrates, inducing leukemia or sarcoma in fish, rodents, cats, and primates.

Note that our reported affinity values are higher than earlier published results for poly(U) (Karpel et al., 1987). This is likely to be the result of a questionable state of metalation and/or oxidation of the zinc finger region in the earlier study in which neither reconstitution with added zinc salt nor special precautions to avoid Cys oxidation were undertaken. While the Cys-rich region identified in retroviral nucleocapsid proteins (Henderson et al., 1981) was proposed to be responsible for Zn(II) chelation (Berg, 1986), controversial findings were reported subsequently that either favored the binding of divalent ions in these regions (Schiff et al., 1988) or ruled against it (Jentoft et al., 1988; Katz & Jentoft, 1989). Solid proof of the occurrence of retroviral zinc finger structures did not arise until solution NMR structures of isolated zinc finger peptides from HIV-1 p7 (South et al., 1989, 1990a,b, 1991), a double zinc finger p7 sequence (Omichinski et al., 1991), and full length HIV-1 p7 (Summers et al., 1992) became available. Ultimately, EXAFS studies showed that stoichiometric quantities of zinc were present in intact retroviruses (Summers et al., 1992; Chance et al., 1992). It is worth noting that p7 NC proteins of HIV-1 carrying altered Cys residues (alkylated, disulfide-bonded, or point-mutated to Ala), rendering them unable to bind metal ions, exhibit a decrease in binding affinity of 1−2 orders of magnitude for a given oligonucleotide sequence (M. A. Urbaneja, J. R. Casas-Finet, et al., unpublished data). A similar effect may be operating for the murine NC homolog studied previously (Karpel et al., 1987).

ODMR Measurements. p10-ZF′ with Poly(U) and Poly-(I). We can conclude at the outset that no effects of nucleic acid binding on the triplet state properties of Trp in the Y ↔ W switched peptide, p10-ZF′, are evident. Not a single criterion that provides evidence for aromatic stacking interactions is present. The phosphorescence lifetime (77 K) of Trp is unaffected as are the apparent individual sublevel decay constants obtained from analysis of the delayed slow-passage spectra at 1.2 K (Table 3). With the exception of $(5\text{-BrdU})_7$dT, to be discussed below, the ZFS parameters of p10-ZF′ as well as the $\lambda_{0,0}$ are unaffected by RNA binding within experimental error (Table 1). The apparent decay constants are unchanged by nucleic acid binding in each case.

Table 2: ODMR Frequencies and Zero-Field Splitting Parameters of p10, the Zinc Finger Peptides p10-ZF and p10-ZF′, and Their Complexes with Nucleic Acids

	$\lvert D\rvert - \lvert E\rvert$[a]		$2\lvert E\rvert$[a]		$\lvert D\rvert + \lvert E\rvert$[a]			
sample	ν_0 (GHz)	$\nu_{1/2}$ (MHz)	ν_0 (GHz)	$\nu_{1/2}$ (MHz)	ν_0 (GHz)	$\nu_{1/2}$ (MHz)	$\lvert D\rvert$ (GHz)	$\lvert E\rvert$ (GHz)
p10	1.716(1)	53(2)	2.495(6)	106(7)	–	–	2.964	1.248
p10 + poly(U)	1.704(2)	61(3)	2.506(16)	149(20)	–	–	2.957	1.253
p10 + poly(I)	1.632(3)	64(2)	2.434(18)	190(22)	–	–	2.849	1.217
p10 + (5-BrdU)$_7$dT	1.658(20)	104(9)	2.527(21)	130(39)	4.120(5)	184(53)	2.889	1.247
p10-ZF	1.715(1)	54(1)	2.519(3)	113(2)	4.225(3)	85(2)	2.970	1.257
p10-ZF + poly(U)	1.692(1)	63(3)	2.486(8)	109(12)	–	–	2.935	1.243
p10-ZF + poly(I)	1.655(3)	59(7)	2.552(19)	127(2)	–	–	2.931	1.276
p10-ZF + (5-BrdU)$_7$dT	1.658(7)	96(5)	2.508(37)	121(6)	–	–	2.912	1.254
p10-ZF′	1.725(3)	60(1)	2.513(7)	125(9)	4.236(3)	83(7)	2.981	1.256
p10-ZF′ + poly(U)	1.718(3)	62(3)	2.515(8)	120(9)	4.254(26)	91(2)	2.986	1.263
p10-ZF′ + poly(I)	1.737(3)	58(3)	2.474(2)	117(13)	4.216(15)	56(9)	2.977	1.238
p10-ZF′ + (5-BrdU)$_7$dT	1.698(1)	68.5(3)	2.533(3)	133(4)	4.177(2)	145(54)	2.938	1.253

[a] The standard deviation (σ) in the last digit is given in parentheses. Values are from Levenberg−Marquardt least-squares fitting of delayed slow-passage ODMR responses at 1.2 K (Wu et al., 1996b).

Table 3: Kinetic Parameters of Trp in p10, Its Zinc Finger Peptides, p10-ZF and p10-ZF′, and Their Complexes with Nucleic Acids

sample	$\lambda_{0,0}$ (nm)	τ (s)[a]	k_x (s^{-1})[b]	k_y (s^{-1})[b]	k_z (s^{-1})[b]	R_{zx}[b]	R_{yx}[b]	R_{zy}[b]
p10	409.2	6.7 (95), 0.68 (5)	0.34(3)	0.083(2)	0.051(5)	0.11(8)	0.15(4)	–
p10 + poly(U)	410.0	6.3 (50), 0.82 (50)	0.40(3)	0.1(1)	0.08(7)	0.17(9)	0.19(9)	–
p10 + poly(I)	413.2	2.7 (59), 0.50 (41)	0.53(1)	0.3(1)	0.086(7)	0.13(1)	0.09(3)	–
p10 + (5-BrdU)$_7$dT	417.6	5.9 (65), 0.42 (34)	0.50(5)	0.32(7)	0.04(1)	0.08(2)	0.2(1)	0.8(2)
p10-ZF	409.4	6.5 (93), 0.83 (7)	0.37(3)	0.19(3)	0.051(10)	0.10(1)	0.26(9)	0.40(4)
p10-ZF + poly(U)	410.4	6.1 (85), 0.77 (15)	0.34(5)	0.10(2)	0.04(1)	0.14(1)	0.29(9)	–
p10-ZF + poly(I)	413.2	4.8 (50), 0.50 (50)	0.45(5)	0.20(11)	0.09(3)	0.15(6)	0.5(2)	–
p10-ZF + (5-BrdU)$_7$dT	418.0	5.4 (57), 0.42 (43)	0.41(3)	0.18(5)	0.06(2)	0.14(2)	0.11(9)	–
p10-ZF′	409.1	6.5 (87), 0.90 (13)	0.35(4)	0.17(2)	0.059(9)	0.114(5)	0.29(4)	0.51(2)
p10-ZF′ + poly(U)	409.3	6.3 (87), 0.56 (13)	0.36(4)	0.22(7)	0.045(13)	0.12(1)	0.35(20)	0.26(8)
p10-ZF′ + poly(I)	408.5	6.4 (89), 0.66 (11)	0.37(6)	0.19(3)	0.077(26)	0.14(4)	0.33(7)	0.7(1)
p10-ZF′ + (5-BrdU)$_7$dT	411.2	6.3 (89), 1.02 (11)	0.33(3)	0.19(2)	0.077(20)	0.153(4)	0.33(11)	0.56(8)

[a] Phosphorescence was measured at 77 K. Pre-exponential terms (in percent) are given in parentheses. [b] Apparent values obtained from Levenberg−Marquardt least-squares analyses of delayed slow-passage ODMR responses at 1.2 K (Wu et al., 1996b). Standard deviations (σ) in the last digit are given in parentheses.

The lack of major nucleic acid binding effects on the triplet state properties of p10-ZF′ is qualitatively evident from a comparison of the conventional slow-passage ODMR spectra in Figure 3. These findings are in complete agreement with the drastic decrease in binding affinity observed by fluorescence measurements on this peptide.

p10 and p10-ZF with Poly(I) and Poly(U). In contrast with p10-ZF′, the triplet state properties of Trp in both p10 and p10-ZF show evidence of stacking interactions.

Binding of Poly(I). A 4 nm red shift of $\lambda_{0,0}$ is induced in both peptides upon binding poly(I). The apparent k_i's (Table 3) increase significantly upon binding p10 to poly(I). The largest relative increase (about 4-fold) occurs in k_y, while k_x increases by about 50%. These increases may occur in the actual decay constants, or they may be the result of increased SLR, which is not considered in the analysis. Although the apparent k_i's perhaps are influenced somewhat by SLR, it can be shown that the increases are largely due to the actual k_i's. The average triplet decay constant is not influenced by SLR but is related to the actual sublevel decay constants by

$$k_{av} = (k_x + k_y + k_z)/3 = 1/\tau_{av}$$

Assuming that the apparent k_i's from Table 3 approximate the actual sublevel decay constants for the p10 complex with poly(I), $\tau_{av} = 3.3 \pm 0.4$ s. This lifetime corresponds rather closely with the major lifetime component in the analysis of the phosphorescence decay at 77 K (2.7 s) that is attributed to Trp. The shorter lifetime component, also observed in the poly(I)−p10-ZF and poly(I)−p10-ZF′ systems, could originate from Tyr and/or from the polynucleotide. Thus, it can be concluded that the effect of poly(I) binding on the triplet state kinetics appears largely in the actual k_i's, rather than the SLR rate constants. It should be noted that the large selective increase in the k_y parameter upon poly(I) binding (bringing it close to k_x) is consistent with poor signal intensity of the delayed slow-passage 2*E* ODMR signal relative to that of the $D - E$ signal (Figure 4). The sublevel populations of T_x and T_y can diverge from each other during decay (and produce ODMR signals), only if their decay constants differ.

Binding of p10 to poly(I) also leads to major effects on the ZFS parameters that are consistent with aromatic stacking interactions. The *D* parameter is reduced by ca. 115 MHz, while a smaller reduction (ca. 31 MHz) occurs in *E*. Such effects, particularly on the *D* parameter, are expected to be caused by stacking interactions as a result of charge transfer character introduced into the triplet state (Haenel & Schweitzer, 1988).

Clearly, binding of p10-ZF to poly(I) results in smaller perturbations of the triplet state than is the case with p10. Although the red shift of the phosphorescence is the same, the apparent decay constants are affected to a smaller extent (Table 3), as are the ZFS parameters (Table 2). *D* is reduced

by barely 40 MHz, while *E* apparently increases by ca. 19 MHz.

Binding of Poly(U). In comparison with poly(I), binding to poly(U) produces only marginal effects on the triplet state properties of p10 and p10-ZF. The phosphorescence red shift induced in each peptide is only ca. 1 nm (Table 3), but this is somewhat above the experimental error of ±0.3 nm. A minor effect on the decay kinetics of the triplet state is apparent only for p10. The apparent decay constants at 1.2 K and the phosphorescence kinetics of p10-ZF at 77 K remain unchanged within experimental error. The ZFS parameters of p10 are virtually unchanged upon binding poly(U), while those of p10-ZF are only slightly affected. The effects observed upon binding of poly(U) are so marginal that we believe they probably are due largely to nonspecific effects of binding rather than to aromatic stacking interactions. These results agree with the moderate affinity measured for p10 to poly(dT) relative to poly(dI), 4.3×10^6 *vs* 6.7×10^7 M^{-1} (Table 1), and the decrease in affinity of 3 orders of magnitude observed for p10-ZF, relative to the full length protein.

Peptide Interactions with (5-BrdU)$_7$dT. Large phosphorescence red shifts (8−9 nm) are induced in both p10 and p10-ZF upon interaction with this octanucleotide, whereas only a minor red shift (2 nm) is induced in p10-ZF′. As far as an external heavy atom effect is concerned, which would be expected from the close approach of Trp to the Br atom, none is detectable, except for a minor effect in the case of p10 (Table 3). The enhancement of the apparent *k*'s is very small in p10; the size of this enhancement is inconsistent with van der Waals contact between Trp and the Br atom. In previous measurements (Lam et al., 1994), we found that binding of p7 to (5-BrdU)$_7$dT reduces the average phosphorescence lifetime of Trp 37 to well below 1 s, in contrast with a τ_{av} of about 4 s for p10, based on the k_i's listed in Table 3. Furthermore, kinetic measurements of the indole phosphorescence in crystalline *p*-dibromobenzene (Smith & Maki, 1993) in which Br atoms are in van der Waals contact with indole yield values for τ_{av} of 0.012 and 0.033 s for two distinguishable indole orientations in the lattice. Stacking interactions of the indole residue of p10 or the zinc finger peptides with 5-BrdU, if they occur, must be minimal in order to avoid van der Waals contacts with the Br atoms.

The effects of (5-BrdU)$_7$dT binding to p10 and p10-ZF on the phosphorescence origin and ZFS, on the other hand, are considerable (Tables 2 and 3). The value of *D*, for instance, is reduced by 75 and 58 MHz in p10 and p10-ZF, respectively, although the value of *E* is unchanged. The phosphorescence and ZFS shifts in p10-ZF′, on the other hand, are considerably smaller. These effects are probably the result of increased polarizability of the Trp environment resulting from the introduction of highly polarizable Br atoms. The decrease in the ZFS is expected from increased polarizability of the environment because of the expansion of the electron cloud that results in reduced magnetic dipole−dipole interactions. In contrast with the heavy atom effect, which drops off precipitously beyond van der Waals contact, these effects of polarizability have a much longer range. The effects of the Br atom polarizability in the absence of a large heavy atom perturbation could indicate that complex formation of p10 and p10-ZF with (5-BrdU)$_7$dT involves an interaction with nucleobases that excludes direct van der Waals contact with Br. This lack of a heavy atom effect is in direct contrast with p7 binding to (5-BrdU)$_7$dT (Lam et al., 1994), where a heavy atom effect consistent with a closer approach to Br is observed. The difference in interaction with the Br atom could stem from the relative location of Trp in the two zinc fingers. In p7, Trp 37 is located between Cys 35 and Cys 38, the position analogous to that occupied by Tyr 28 in p10, rather that adjacent to His 34, which is the location of Trp in p10. This places the Trp residues in p7 and p10 on opposite sides of the zinc finger. The phosphorescence red shift induced in p10 by (5-BrdU)$_7$dT, however, is only 1 nm less than in p7 (8.4 *vs* 9.4 nm). The observation that the phosphorescence red shift and reduction of the ZFS are smaller in p10-ZF′ than in p10-ZF is consistent with a larger distance between the Trp site and the nucleobases in this Y ↔ W switched peptide than is found in p10 and p10-ZF complexes.

A detailed account describing the effect of demetalation and various salt concentrations on wild-type and point-mutated MoMuLV p10 is being prepared for publication elsewhere. For d(UG)$_4$, the sequence with the highest affinity for p10 used in that study, the binding constant at 150 mM NaCl is 7.9×10^5 M^{-1} ($\log K_{app} = 5.9$). Most oligonucleotides used in the present study would exhibit dissociation constants in the micromolar to millimolar range at physiological osmolarity. Note, however, that positive binding cooperativity is expected in the association of the polyprotein Gag precursor (Pr-Gag65) with RNA due to the occurrence of protein−protein interactions. Marginal cooperativity is observed in the binding of processed p10 to long polynucleotides.

CONCLUSIONS

Fluorescence titrations, phosphorescence, and ODMR measurements on p10, p10-ZF, and p10-ZF′ interacting with several nucleic acids have been carried out. Among the nucleic acids investigated by fluorescence, poly(dI) is found to bind with highest affinity to p10, while p10-ZF binds with lesser affinity, and no binding of p10-ZF′ to this lattice is detectable. It appears that high-affinity binding requires that Tyr and Trp be in their native positions in the zinc finger. Their interchange leads to a severe loss of binding affinity. Furthermore, polynucleotides appear to bind with higher affinity than octanucleotides, i.e., poly(dI) > (dI)$_8$. Also, a full length NC protein binds with greater affinity than the 24−41 peptide studied. The inosine lattice provides tighter binding than the uracil (or thymine) lattice, (dI)$_8$ > (dT)$_8$ and (dU)$_7$dT (Table 1), although binding of p10 to each of these lattices is observed. From the ODMR and phosphorescence measurements, binding of p10 to poly(U) produces hardly any effects that can be associated with aromatic stacking interactions, in sharp contrast to the effects of poly(I) binding. This comparison suggests that the difference in binding affinity (about a factor of 15−20 in K_{app} for I *vs* T lattices, Table 1) may be due to the contribution of aromatic stacking interactions to the free energy of association. The absence of an external heavy atom effect in the interaction of p10 with (5-BrdU)$_7$dT demonstrates that there is no van der Waals contact between Trp and the Br atoms. Any aromatic interactions are sufficiently minor that contact is avoided. This is consistent with the absence of aromatic stacking effects in p10 complexes of poly(U), mentioned

above. Shifts in the phosphorescence wavelength and in the ZFS of Trp are attributed to general polarizability effects caused by the Br atom; these are even present, but to a lesser extent, in p10-ZF′ which is not observed to interact with any of the other nucleic acids (Tables 2 and 3).

REFERENCES

Alfredson, T. V., Maki, A. H., & Waring, M. J. (1991) *Biochemistry 30*, 9665−9675.

Berg, J. (1986) *Science 232*, 485−487.

Bess, J. W., Jr., Powell, P. J., Issaq, H. J., Schumack, L., Grimes, M. K., Henderson, L. E., & Arthur, L. O. (1992) *J. Virol. 66*, 840−847.

Casas-Finet, J. R., Khamis, M. I., Maki, A. H., Ruvolo, P. P., & Chase, J. W. (1987) *J. Biol. Chem. 262*, 8574−8583.

Casas-Finet, J. R., Toulmé, J.-J., Santus, R., & Maki, A. H. (1988a) *Eur. J. Biochem. 172*, 641−646.

Casas-Finet, J. R., Jhon, N.-I., Khamis, M. I., Maki, A. H., Ruvolo, P. P., & Chase, J. W. (1988b) *Eur. J. Biochem. 178*, 101−107.

Casas-Finet, J. R., Jhon, N.-I., & Maki, A. H. (1988c) *Biochemistry 27*, 1172−1178.

Chance, M. R., Sagi, I., Wirt, M. D., Frisbie, S. M., Scheuring, E., Chen, E., Bess, J. W., Jr., Henderson, L. E., Arthur, L. O., South, T. L., Perez-Alvarado, G., & Summers, M. F. (1992) *Proc. Natl. Acad. Sci. U.S.A. 89*, 10041−10045.

Co, T., & Maki, A. H. (1978) *Biochemistry 17*, 182−186.

Darlix, J.-L., Lapadat-Tapolsky, M., de Rocquigny, H., & Roques, B. P. (1995) *J. Mol. Biol. 254*, 523−537.

DeStefano, J. J. (1995) *Arch. Virol. 140*, 1775−1789.

DeStefano, J. J., Buiser, R. G., Mallaber, L. M., Fay, P. J., & Bambara, R. A. (1992) *Biochim. Biophys. Acta 1131*, 270−280.

Dib-Haij, F., Khan, R., & Giedroc, D. P. (1993) *Protein Sci. 2*, 231−243.

Gallay, P., Swingler, S., Aiken, C., & Trono, D. (1995) *Cell 80*, 379−388.

Gorelick, R. J., Henderson, L. E., Hanser, J. P., & Rein, A. (1988) *Proc. Natl. Acad. Sci. U.S.A. 85*, 8420−8424.

Gorelick, R. J., Nigida, S. M., Jr., Bess, J. W., Jr., Arthur, L. O., Henderson, L. E., & Rein, A. (1991) *AIDS Res. Hum. Retroviruses 7*, 194.

Gorelick, R. J., Chabot, D. J., Rein, A., Henderson, L. E., & Arthur, L. O. (1993) *J. Virol. 67*, 4027−4036.

Gorelick, R. J., Chabot, D. J., Ott, D. E., Gagliardi, T. D., & Arthur, L. O. (1996) *J. Virol. 70*, 2593−2597.

Haenel, M. W., & Schweitzer, D. W. (1988) *Adv. Chem. Ser. 217*, 333−355.

Henderson, L. E., Copeland, T. D., Sowder, R. C., Smythers, G. W., & Oroszlan, S. (1981) *J. Biol. Chem. 256*, 8400−8406.

Henderson, L. E., Sowder, R., Copeland, T. D., Smythers, G., & Oroszlan, S. (1984) *J. Virol. 52*, 492−500.

Herschlag, D., Khosia, M., Tsuchihashi, Z., & Karpel, R. L. (1994) *EMBO J. 13*, 2913−2924.

Hoff, A. J. (1989) in *Advanced EPR. Applications in Biology & Biochemistry* (Hoff, A. J., Ed.) pp 633−684, Elsevier, Amsterdam.

Jentoft, J. E., Smith, L. M., Fu, X., Johnson, M., & Leis, J. (1988) *Proc. Natl. Acad. Sci. U.S.A. 85*, 7094−7098.

Ji, X., Klarmann, G. J., & Preston, B. D. (1996) *Biochemistry 35*, 132−143.

Karpel, R. L., Henderson, L. E., & Oroszlan, S. (1987) *J. Biol. Chem. 262*, 4961−4967.

Katz, R. A., & Jentoft, J. E. (1989) *BioEssays 11*, 176−181.

Khamis, M. I., & Maki, A. H. (1986) *Biochemistry 25*, 5865−5872.

Khamis, M. I., Casas-Finet, J. R., Maki, A. H., Murphy, J. B., & Chase, J. W. (1987) *J. Biol. Chem. 262*, 10938−10945.

Khan, R., & Giedroc, D. P. (1992) *J. Biol. Chem. 267*, 6689−6695.

Kumar, N. V., & Govil, G. (1984) *Biopolymers 23*, 2009−2024.

Lam, W. -C., Maki, A. H., Casas-Finet, J. R., Erickson, J. W., Sowder, R. C., II, & Henderson, L. E. (1993) *FEBS Lett. 328*, 45−48.

Lam, W.-C., Maki, A. H., Casas-Finet, J. R., Erickson, J. W., Kane, B. P., Sowder, R. C., II, & Henderson, L. E. (1994) *Biochemistry 33*, 10693−10700.

Lapadat-Tapolsky, M., Pernelle, C., Borie, C., & Darlix, J.-L. (1995) *Nucleic Acids Res. 23*, 2434−2441.

Long, C. W., Henderson, L. E., & Oroszlan, S. (1980) *Virology 104*, 491−496.

Maki, A. H. (1984) in *Biological Magnetic Resonance* (Berliner, L., & Reuben, J., Eds.) Vol. 6, pp 187−293, Plenum Press, New York.

Maki, A. H. (1995) *Methods Enzymol. 246*, 610−638.

Maki, A. H., Alfredson, T. V., & Waring, M. J. (1992) *Proc. SPIE-Int. Soc. Opt. Eng. 1640*, 485−497.

Mascotti, D. P., & Lohman, T. M. (1993) *Biochemistry 32*, 10568−10579.

Mçric, C., & Goff, S. P. (1989) *J. Virol. 63*, 1558−1569.

Michelson, A. M., Dondon, J., & Grunberg-Manago, M. (1962) *Biochim. Biophys. Acta 55*, 529−540.

Omichinski, J. G., Clore, G. M., Sakaguchi, K., Appella, E., & Gronenborn, A. M. (1991) *FEBS Lett. 292*, 25−30.

Pellska, J. A., Balasubramanian, S., Giedroc, D. P., & Benkovic, S. J. (1994) *Biochemistry 33*, 13817−13823.

Prats, A.-C., Housset, V., de Billy, G., Cornille, F., Prats, H., Roques, B., & Darlix, J.-L. (1991) *Nucleic Acids Res. 19*, 3533−3541.

Rodriguez-Rodriguez, L., Tsuchihashi, Z., Fuentes, G. M., Bambara, R. A., & Fay, P. J. (1995) *J. Biol. Chem. 270*, 15005−15011.

Schiff, L. A., Nibert, M. L., & Fields, B. N. (1988) *Proc. Natl. Acad. Sci. U.S.A. 85*, 4195.

Schmalzbauer, E., Strack, B., Dannull, J., Guehmann, S., & Moelling, K. (1996) *J. Virol. 70*, 771−777.

Shinnick, T. M., Lerner, R. A., & Sutcliff, J. G. (1981) *Nature 293*, 543−548.

Smith, C., & Maki, A. H. (1993) *J. Phys. Chem. 97*, 997−1003.

South, T. L., Kim, B., & Summers, M. F. (1989) *J. Am. Chem. Soc. 111*, 395−396.

South, T. L., Blake, P. R., Sowder, R. C., Arthur, L. O., Henderson, L. E., & Summers, M. F. (1990a) *Biochemistry 29*, 7786−7789.

South, T. L., Kim, B., Hare, D. R., & Summers, M. F. (1990b) *Biochem. Pharmacol. 40*, 123−129.

South, T. L., Blake, P. R., Hare, D. R., & Summers, M. F. (1991) *Biochemistry 30*, 6342−6349.

Summers, M. F., Henderson, L. E., Chance, M. R., Bess, J. W., Jr., South, T. L., Blake, P. R., Sagi, I., Perez-Alvarado, G., Sowder, R. C., III, Hare, D. R., & Arthur, L. O. (1992) *Protein Sci. 1*, 563−574.

Tsao, D. H. H., Casas-Finet, J. R., Maki, A. H., & Chase, J. W. (1989) *Biophys. J. 55*, 927−936.

Tsuchihashi, Z., & Brown, P. O. (1994) *J. Virol. 68*, 5863−5870.

Wu, J. Q., Ozarowski, A., & Maki, A. H. (1996a) *J. Magn. Reson., Ser. A 119*, 82−89.

Wu, J. Q., Ozarowski, A., Davis, S. K., & Maki, A. H. (1996b) *J. Phys. Chem. 100*, 11496−11503.

You, J. C., & McHenry, C. S. (1994) *J. Biol. Chem. 269*, 31491−31495.

Zang, L.-H., Maki, A. H., Murphy, J. B., & Chase, J. W. (1987) *Biophys. J. 52*, 867−872.

BI962951O